Geomechanics and Engineering, *Vol. 22, No. 1 (2020) 65-80*
DOI: https://doi.org/10.12989/gae.2020.22.1.065

Impact of the homogenization models on the thermoelastic response of FG plates on variable elastic foundation

Mohamed Ali Rachedi[1,2], Samir Benyoucef*[1], Abdelhakim Bouhadra[1,2a], Rabbab Bachir Bouiadjra[1,3a], Mohamed Sekkal[1a] and Abdelkader Benachour[1b]

[1]*Material and Hydrology Laboratory, University of Sidi Bel Abbes, Faculty of Technology, Algeria*
[2]*Department of Civil Engineering, Faculty of Science and Technology, University of Abbés Laghrour Khenchela, Algeria*
[3]*Department of Civil Engineering, University Mustapha Stambouli of Mascara, Algeria*

(Received March 31, 2020, Revised April 30, 2020, Accepted May 23, 2020)

Abstract. This paper presents a theoretical investigation on the response of the thermo-mechanical bending of FG plate on variable elastic foundation. A quasi-3D higher shear deformation theory is used that contains undetermined integral forms and involves only four unknowns to derive. The FG plates are supposed simply supported with temperature-dependent material properties and subjected to nonlinear temperature rise. Various homogenization models are used to estimate the effective material properties such as temperature-dependent thermoelastic properties. Equations of motion are derived from the principle of virtual displacements and Navier's solution is used to solve the problem of simply supported plates. Numerical results for deflections and stresses of FG plate with temperature-dependent material properties are investigated. It can be concluded that the proposed theory is accurate and simple in solving the thermoelastic bending behavior of FG thick plates.

Keywords: quasi-3D solution; FG thick plates; homogenization models; temperature-dependent material; thermo-mechanical bending

1. Introduction

In modern industries, the use of advanced composite materials in engineering applications are increased because of their ability to control and to withstand stresses caused by thermo-mechanical loading. Functionally graded materials (FGM) belong to this new generation of advanced composite materials in which the thermal and mechanical properties change gradually in one or more directions according to the volume fraction of its constituent materials (Lal *et al.* 2017, Almitani 2018, Rezaiee-Pajand *et al.* 2018, Bessaim *et al.* 2018, Faleh *et al.* 2018, Ahmed *et al.* 2019, Akbaş 2019, Sayyad and Ghumare 2019, Fenjan *et al.* 2019a, Ramirez *et al.* 2019, Esmaeili and Beni 2019, Ahmed *et al.* 2019, Al-Maliki *et al.* 2020,Gafour *et al.* 2020, Kar and Panda 2020). With the massive application of FGM in modern technologies such as energy sources, aerospace, automotive, nuclear reactor, mechanical, nanostructures, civil, electronic and shipbuilding industries (Sedighi *et al.* 2015, Batou *et al.* 2019, Chaabane *et al.* 2019, Berghouti *et al.* 2019, Salah *et al.* 2019, Hellal *et al.* 2019, Boulefrakh *et al.* 2019, Tlidji *et al.* 2019, Boukhlif *et al.* 2019, Balubaid *et al.* 2019, Al-Maliki *et al.* 2020, Kaddari *et al.* 2020, Rahmani *et al.* 2020), many researchers have focused on the study and development of theories relating to the behavior of FG structures and particularly thermo-mechanical analysis. Various FGM plate theories have been developed to predict the structures behavior in the past decades, such as classical plate theory (CPT), the first shear deformation theory (FSDT) and the High order Shear Deformation plate Theory (HSDT). The FSDT was used by Cong *et al.* (2015) to investigate the nonlinear stability of eccentrically stiffened moderately thick FG plates with temperature-dependent material properties subjected to in plane compressive and thermo-mechanical load. In the same framework, Ping *et al.* (2014) have employed the local meshless method with moving Kriging interpolation for geometrically nonlinear analysis of functionally graded plates in thermal environments. By using the third order shear deformation theory (TSDT), the same researchers (Cong *et al.* 2017) studied the nonlinear dynamic response of stiffened FGM plate in thermal medium subjected to mechanical and thermal loads. They consider the temperature-dependent materials properties. Ghiasian *et al.* (2014) investigated the thermal buckling of shear deformable temperature-dependent circular/ annular FGM plates. Zhu *et al.* (2014) analyze the thermomechanical behavior of moderately thick FGM plates using a local meshless method with Kriging interpolation technique. Trinh *et al.* (2017) studied the static bending, buckling and free vibration of FG sandwich microplates subjected to thermomechanical loading on the base of the modified couple stress theory by using Navier solutions. Li *et al.* (2016, 2017) use the four-variable refined plate theory to investigate the thermomechanical bending of FG sandwich plates. Using the HSDT, Kar *et al.* (2016) studied the linear/nonlinear deformation of FG

*Corresponding author, Professor
E-mail: samir.benyoucef@gmail.com
[a]Ph.D.
[b]Professor

ISSN: 2005-307X (Print), 2092-6219 (Online)

spherical shell panel subjected to thermomechanical load. They included the nonlinear geometry. Parida and Mohanty (2017) performed a mathematical model to investigate the nonlinear free vibration of FG skew plate in thermal environment. They present a formulation based on the HSDT in conjunction with Green-Lagrange-type geometric nonlinearity. Yoosefian *et al.* (2020) investigated the nonlinear thermo-elastic bending of circular/annular symmetric FGM sandwich plates. Zarga *et al.* (2019) presented an analysis of the thermo-mechanical bending of FG sandwich plates by a quasi-3D shear deformation theory. Tounsi *et al.* (2020) presented a four variable trigonometric integral plate theory for hygro-thermo-mechanical bending analysis of FG ceramic-metal plates resting on a two-parameter elastic foundation. Boussoula *et al.* (2020) developed a simple nth-order shear deformation theory for thermomechanical bending analysis of different configurations of FG sandwich plates. It should be noted also that the thermal effects is examined for laminated structures (Abualnour *et al.* 2019, Belbachir *et al.* 2019 and 2020).

Plates resting on elastic foundation were discussed through a number of researchers using several techniques. Trinh and Kim (2018) presented a theoretical procedure based on the FSDT to study the buckling loads and post-buckling equilibrium path of the moderately thick FG sandwich shells supported by elastic foundation and subjected to thermomechanical loads. Nguyen *et al.* (2016) presented an analytical solution to study the thermal stability of eccentrically stiffened FGM plate on elastic foundation subjected to mechanical, thermal and thermomechanical load. They use the Reddy third order shear deformation plate theory (TSDT). Using the same theory, Nguyen *et al.* (2018) investigated the nonlinear thermo-mechanical response of imperfect Sigmoid FGM circular cylindrical shells surrounded on elastic foundations. Kolahchi *et al.* (2016) investigated the nonlinear dynamic stability behavior of polymeric temperature dependent viscoelastic plates reinforced by SWCNTs resting on orthotropic temperature dependent elastomeric medium.

Most of research on FG plates or beams has been undertaken with structures resting on elastic foundations with constant modules. However, studies on structures based on variable elastic foundations are limited in the literature. Pradhan and Murmu (2009) illustrated the thermomechanical vibration analysis of FG beams and FG sandwich (FGSW) beams resting on variable elastic foundations. Sobhy (2015) presented a 2D theory based on the sinusoidal shear deformation plate theory to study the thermomechanical bending of FG plates with various boundary conditions and resting on variable elastic foundation. Attia *et al.* (2018) developed a 2D simple HSDT for thermo mechanical bending of temperature-dependent FG plates on variable elastic foundation.

Most research on FGM uses the rules of mixture to assess the effective material properties; an appropriate micromechanical model must be applied to accurately estimate the effective multiphysical properties. Among the works in the literature, a few standard micromechanical models could be remarked (Nemati and Mahmoodabadi 2019), as Voigt (1889), Reuss (1929) and Mori-Tanaka (1973). Benyoucef and his co-workers (Bachir Bouiadjra *et al.* 2018, Yahiaoui *et al.* 2018) have presented some research on the effect of micromechanical models on the response of FG structures.

As shown in the above literature review, the thermoelastic analysis of FG structures has received little attention. It is known that FG structures are often applied in severe thermal environments and the understanding of their thermoelastic performance is in great demand. This work is done to meet demand.

As far as authors known, in literature there is no available work treating the effect of micromechanical models on the thermoelastic response of FG plates resting on variable elastic foundation and using a quasi-3D plate theory. Thus, the present paper aims to improve the 2D theory developed by Attia *et al.* (2018) by including the stretching effect to study the effect of several micromechanical models on the thermomechanical response of FG thick plate resting on variable elastic foundation. The highlight of the used theory is that contains undetermined integral terms and involves a reduced number of variables and governing equations than the conventional quasi-3D theories. Different micromechanical models are assessed to determine the effective material properties of FG plates. The effects of these models, the thermomechanical loading and the elastic foundation on the overall response of the plates will be discussed in detail via a parametric study.

2. Effective properties of FGMs

2.1 Temperature-dependent materials

FGMs are composite materials most often made of ceramic and metal. Since they are used in high temperature environments, the constituents of FGM may possess temperature-dependent properties (Reddy and Chin 1998). Therefore, the properties including Young's modulus E, thermal expansion α and thermal conductivity k are assumed to be temperature-dependent and are expressed as function of temperature (Attia *et al.* 2018, Nemati and Mahmoodabadi 2019):

$$P_f(T,z) = P_0\left(P_{-1}T(z)^{-1} + 1 + P_1T(z) + P_2T(z)^2 + P_3T(z)^3\right) \quad (1)$$

P_{-1}, P_0, P_1, P_2 and P_3 are the coefficients of temperature T expressed in Kelvin and are unique to the constituent materials. ΔT is rise temperature through the thickness direction. $P_f(T,z)$ it is an effective property. In our case, it can be either metal or ceramic. The values of each of the coefficients appearing in the preceding equation are listed in Table 1.

2.2 Micromechanical models

Unlike traditional microstructures, in FGMs the material properties are spatially varying, which is not trivial for a

micromechanics model (Jaesang and Addis 2014).

A number of micromechanics models have been proposed for the determination of effective properties of FGMs.

In this work, the Voigt, Reuss, LRVE, Tamura and Mori-Tanaka models are employed to determine the effective material properties of the FG plate.

2.2.1 Voigt model

The Voigt model is relatively simple; this model is frequently used in most FGM analyses estimates properties of FGMs as (Mishnaevsky 2007, Zimmerman 1994):

$$P(T,z) = P_c(T,z)\,V(z) + P_m(T,z)\big(1-V(z)\big) \tag{2}$$

2.2.2 Reuss model

Reuss assumed the stress uniformity through the material and obtained the effective properties as (Mishnaevsky 2007, Zimmerman 1994):

$$P(T,z) = \frac{P_c(T,z)\,P_m(T,z)}{P_c(T,z)\big(1-V(z)\big) + P_m(T,z)V(z)} \tag{3}$$

2.2.3 Tamura model

The Tamura model uses actually a linear rule of mixtures, introducing one empirical fitting parameter known as "stress-to-strain transfer" (Gasik 1995, Zuiker 1995)

$$q = \frac{\sigma_1 - \sigma_2}{\varepsilon_1 - \varepsilon_2} \tag{4}$$

Estimate for q=0 correspond to Reuss rule and with $q = \pm\infty$ to the Voigt rule, being invariant to the consideration of with phase is matrix and which is particulate. The effective property is found as:

$$P(T,z) = \frac{(1-V(z))\,P_m(T,z)\big(q - P_c(T,z)\big) + V(z)\,P_c(T,z)\big(q - P_m(T,z)\big)}{(1-V(z))\big(q - P_c(T,z)\big) + V(z)\big(q - P_m(T,z)\big)} \tag{5}$$

2.2.4 Description by a representative volume element (LRVE)

The LRVE is developed based on the assumption that the microstructure of the heterogeneous material is known. The input for the LRVE for the deterministic micromechanical framework is usually volume average or ensemble average of the descriptors of the microstructures. The effective property is expressed as follows by the LRVE method (Akbarzadeh *et al.* 2015):

$$P(T,z) = P_m(T,z)\left(1 + \frac{V(z)}{FE - \sqrt[3]{V(z)}}\right) \qquad FE = \frac{1}{1 - \frac{P_m(T,z)}{P_c(T,z)}} \tag{6}$$

2.2.5 Mori-Tanaka model

According to Mori–Tanaka homogenization scheme, the effective Bulk Modulus (K) and the effective shear modulus (G) are given by Mori and Tanaka (1973):

$$P(T,z) = P_m(T,z) + \big(P_c(T,z) - P_m(T,z)\big)\times \left(\frac{V_C}{1 + (1-V_C)\big(P_c(T,z)/P_c(T,z) - 1\big)(1+\upsilon)/(3-3\upsilon)}\right) \tag{7a}$$

where

$$V_C = \left(0{,}5 + \frac{z}{h}\right)^p \tag{7b}$$

In all models outlined above, the subscripts c and m refer to the ceramic and metal respectively and $P(T,z)$ it's a property that can be, Young's modulus E, thermal expansion α or thermal conductivity k of the FG plate.

The volume fractions of the ceramic and metal phases are related by $V_C + V_m = 1$, and V_C is expressed as:

$$V_C = \left(0{,}5 + \frac{z}{h}\right)^p \qquad p \geq 0 \tag{8}$$

3. Theoretical developments

Consider a rectangular FG plate, with total thickness h, length a, and width b, referred to the rectangular Cartesian coordinates (x, y, z), as shown in Fig. 1.

The plate is assumed to rest on a two parameter elastic foundation which consists of closely spaced springs interconnected through a shear layer made of incompressible vertical elements, which deform only by transverse shear.

The mechanical characteristics of the plate are assumed to be varied according to is thickness.

3.1 Kinematics and strains

The displacement field satisfying the conditions of transverse shear stresses (and hence strains) vanishing at (x, y, ±h/2) on the outer (top) and inner (bottom) surfaces of the plate, is given as follows (Achouri *et al.* 2019, Khiloun *et al.* 2019, Boutaleb *et al.* 2019, Sahla *et al.* 2019):

$$\begin{aligned} u(x,y,z) &= u_0(x,y) - z\frac{\partial w_0}{\partial x} + k_1\, f(z)\int \theta(x,y)\,dx \\ v(x,y,z) &= v_0(x,y) - z\frac{\partial w_0}{\partial y} + k_2\, f(z)\int \theta(x,y)\,dy \\ w(x,y,z) &= w_0(x,y) + g(z)\theta(x,y) \end{aligned} \tag{9}$$

where $k_1 = \alpha^2$, $k_2 = \beta^2$, $u_0; v_0; w_0; \theta$; are four unknown displacements of the mid-plane of the plate.

The coefficient k_1 and k_2 depends on the geometry. It can be seen that the kinematic in Eq. (9) introduces only four unknowns $(u, v_0, w_0 \text{ and } \theta)$ with considering the thickness stretching effect.

The shape function $f(z)$ is given as follows:

$$f(z) = z\left(1 - \frac{4z^2}{3h^2}\right) \tag{10a}$$

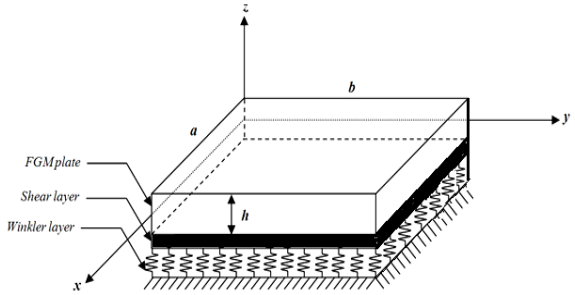

Fig. 1 Coordinate system and geometry for rectangular FG plates on elastic foundation

and

$$g(z)=\frac{2}{12}\frac{df(z)}{dz} \tag{10b}$$

The strain- displacement expressions, based on the formulation, are written under following compact form:

$$\begin{Bmatrix}\varepsilon_x\\ \varepsilon_y\\ \gamma_{xy}\end{Bmatrix}=\begin{Bmatrix}\varepsilon_x^0\\ \varepsilon_y^0\\ \gamma_{xy}^0\end{Bmatrix}+z\begin{Bmatrix}k_x^b\\ k_y^b\\ k_{xy}^b\end{Bmatrix}+f(z)\begin{Bmatrix}k_x^s\\ k_y^s\\ k_{xy}^s\end{Bmatrix}$$
$$\begin{Bmatrix}\gamma_{yz}\\ \gamma_{xz}\end{Bmatrix}=f'(z)\begin{Bmatrix}\gamma_{yz}^0\\ \gamma_{xz}^0\end{Bmatrix}+g(z)\begin{Bmatrix}\gamma_{yz}^1\\ \gamma_{xz}^1\end{Bmatrix},\quad \varepsilon_z=g'(z)\,\varepsilon_z^0 \tag{11}$$

where

$$\begin{Bmatrix}\varepsilon_x^0\\ \varepsilon_y^0\\ \gamma_{xy}^0\end{Bmatrix}=\begin{Bmatrix}\frac{\partial u_0}{\partial x}\\ \frac{\partial v_0}{\partial y}\\ \frac{\partial u_0}{\partial y}+\frac{\partial v_0}{\partial x}\end{Bmatrix},\quad \begin{Bmatrix}k_x^b\\ k_y^b\\ k_{xy}^b\end{Bmatrix}=\begin{Bmatrix}-\frac{\partial^2 w_0}{\partial x^2}\\ -\frac{\partial^2 w_0}{\partial y^2}\\ -2\frac{\partial^2 w_0}{\partial x\partial y}\end{Bmatrix}, \tag{12a}$$

$$\begin{Bmatrix}k_x^s\\ k_y^s\\ k_{xy}^s\end{Bmatrix}=\begin{Bmatrix}k_1\theta\\ k_2\theta\\ k_1\frac{\partial}{\partial y}\int\theta\,dx+k_2\frac{\partial}{\partial x}\int\theta\,dy\end{Bmatrix} \tag{12b}$$

$$\begin{Bmatrix}\gamma_{yz}^0\\ \gamma_{xz}^0\end{Bmatrix}=\begin{Bmatrix}k_2\int\theta\,dy\\ k_1\int\theta\,dx\end{Bmatrix},\quad \begin{Bmatrix}\gamma_{yz}^1\\ \gamma_{xz}^1\end{Bmatrix}=\begin{Bmatrix}\frac{\partial\theta}{\partial y}\\ \frac{\partial\theta}{\partial x}\end{Bmatrix}\varepsilon_z^0=\theta$$

The integrals used in the above equations shall be resolved by a Navier type method and can be given as follows:

$$\frac{\partial}{\partial y}\int\theta\,dx=A'\frac{\partial^2\theta}{\partial x\partial y},\quad \frac{\partial}{\partial x}\int\theta\,dy=B'\frac{\partial^2\theta}{\partial x\partial y},$$
$$\int\theta\,dx=A'\frac{\partial\theta}{\partial x},\quad \int\theta\,dy=B'\frac{\partial\theta}{\partial y} \tag{13a}$$

where the coefficients A' and B' are expressed according to the type of solution used, in this case via Navier. Therefore, A', B', k_1 and k_2 are expressed as follows:

$$A'=-\frac{1}{\alpha^2},\quad B'=-\frac{1}{\beta^2},\quad k_1=\alpha^2,\quad k_2=\beta^2 \tag{13b}$$

where α and β are used in Eq. (35).

3.2 Constitutive relations

The linear constitutive relations of a FG plate can be expressed as

$$\begin{Bmatrix}\sigma_x\\ \sigma_y\\ \sigma_z\\ \tau_{yz}\\ \tau_{xz}\\ \tau_{xy}\end{Bmatrix}=\begin{bmatrix}C_{11}&C_{12}&C_{13}&0&0&0\\ C_{12}&C_{22}&C_{23}&0&0&0\\ C_{13}&C_{23}&C_{33}&0&0&0\\ 0&0&0&C_{66}&&\\ 0&0&0&&C_{55}&\\ 0&0&0&&&C_{44}\end{bmatrix}\begin{Bmatrix}\varepsilon_x-\alpha\Delta T\\ \varepsilon_y-\alpha\Delta T\\ \varepsilon_z-\alpha\Delta T\\ \gamma_{xy}\\ \gamma_{yz}\\ \gamma_{xz}\end{Bmatrix} \tag{14}$$

The C_{ij} (i,j=1,2,4,5,6) expressions in terms of engineering constants are given below

$$C_{ii}=\frac{(1-\nu(z,T))\lambda(z,T)}{\nu(z,T)},\quad (i=1,2,3). \tag{15a}$$

$$C_{ij}=\lambda(z,T),\quad (i,j=1,2,3). \tag{15b}$$

$$C_{ii}=\mu(z,T),\quad (i=4,5,6). \tag{15c}$$

$$\lambda(z)=\frac{E(z,T)}{(1-2\nu(z,T))(1+\nu(z,T))} \tag{15d}$$

$$\mu(z)=\frac{E(z,T)}{2(1+\nu(z,T))} \tag{15e}$$

The plate is assumed to rest on two-parameter elastic foundation model, which consists of closely spaced springs interconnected through a shear layer made of incompressible vertical elements, which deform only by transverse shear. The response equation of this foundation is given by:

$$R(x,y)=\overline{K}(x)\,w(x,y)+\overline{G}\,\nabla^2 w(x,y) \tag{16}$$

where R is the density of the reaction force of elastic foundation, $\overline{K}$ is Winkler parameter depended on x only. It is assumed to be linear, parabolic or sinusoidal (Sobhy 2015, Attia *et al.* 2018, Pradhan and Murmu 2009):

$$\overline{K}(x)=\frac{J_1h^3}{a^4}\begin{cases}1+\xi\frac{x}{a} & \textit{Linear}\\ 1+\xi(\frac{x}{a})? & \textit{Parabolic}\\ 1+\xi\sin(\pi\frac{x}{a}) & \textit{Sinusoidal}\end{cases} \tag{17}$$

in which J_1 is a constant and ξ is a varied parameter. G is

the shear layer foundation stiffness ∇^2 is the Laplace operator in x and y, and w is the deflection of the plate.

Note that, if ξ=0, the elastic foundation becomes Pasternak foundation and if the shear layer foundation stiffness is neglected, the Pasternak foundation becomes the Winkler foundation.

3.3 Equations of motion

The principle of virtual work is here in utilized to determine the equations of motion.

The variation of strain energy of the plate is calculated by (Draiche *et al.* 2019, Chikr *et al.* 2020, Refrafi *et al.* 2020):

$$\begin{aligned}\delta U = \int_A [&N_x\delta\varepsilon_x^0 + N_y\delta\varepsilon_y^0 + N_z\delta\varepsilon_z^0 + N_{xy}\delta\gamma_{xy}^0 + \\ &M_x^b\delta k_x^b + M_y^b\delta k_y^b + M_{xy}^b\delta k_{xy}^b + M_x^s\delta k_x^s + M_y^s\delta k_y^s \\ &+M_{xy}^s\delta k_{xy}^s + Q_{yz}^S\delta\gamma_{yz}^0 + S_{yz}^S\delta\gamma_{yz}^1 + Q_{xz}^S\delta\gamma_{xz}^0 \\ &+S_{xz}^S\delta\gamma_{xz}^1]dA = 0\end{aligned} \tag{18}$$

where A is the surface; and stress resultants N, M, Q, and S are defined by and stiffness components are expressed as:

$$\begin{Bmatrix} N_x & N_y & N_{xy} \\ M_x^b & M_y^b & M_{xy}^b \\ M_x^s & M_y^s & M_{xy}^s \end{Bmatrix} = \int_{-h/2}^{h/2} (\sigma_x,\sigma_y,\tau_{xy}) \begin{Bmatrix} 1 \\ z \\ f(z) \end{Bmatrix} dz \tag{19}$$

$$N_z = \int_{-h/2}^{h/2} \sigma_z \; g'(z)\, dz \tag{20a}$$

$$(S_{xz}^s, S_{yz}^s) = \int_{-h/2}^{h/2} (\tau_{xz},\tau_{yz})\; g(z)\, dz \tag{20b}$$

$$(Q_{xz}^s, Q_{yz}^s) = \int_{-h/2}^{h/2} (\tau_{xz},\tau_{yz})\; f'(z)\, dz \tag{20c}$$

The variation of potential energy of the applied loads can be expressed as

$$\delta V = -\int_A q\delta(w_0(x,y) + g(z)\theta(x,y))dA \tag{21}$$

The variation of potential energy of the foundation can be expressed as

$$\delta U_R = \int_A R\delta(w_0(x,y) + g(z)\theta(x,y))dA \tag{22}$$

Substituting the expressions of δU, δV and δU_R :

$$\begin{aligned}\delta U - \delta V + \delta U_R = &\int_A [N_x\delta\varepsilon_x^0 + N_y\delta\varepsilon_y^0 + N_z\delta\varepsilon_z^0 + N_{xy}\delta\gamma_{xy}^0 \\ &+M_x^b\delta k_x^b + M_y^b\delta k_y^b + M_{xy}^b\delta k_{xy}^b + M_x^s\delta k_x^s + M_y^s\delta k_y^s \\ &+M_{xy}^s\delta k_{xy}^s + Q_{yz}^S\delta\gamma_{yz}^0 + S_{yz}^S\delta\gamma_{yz}^1 + Q_{xz}^S\delta\gamma_{xz}^0 + S_{xz}^S\delta\gamma_{xz}^1]dA \\ &-\int_A q\delta w_0 dA - \int_A qg(z)\delta\theta dA + \int_A R\delta w_0 dA + \int_A Rg(z)\delta\theta dA = 0\end{aligned} \tag{23}$$

Integrating by parts, and collecting the coefficients of δu_0, δv_0, δw_0, and $\delta\theta$, and the following equations of motion of the plate are obtained:

$$\begin{aligned}&\delta u_0: \quad \frac{\partial N_x}{\partial x} + \frac{\partial N_{xy}}{\partial y} = 0 \\ &\delta v_0: \quad \frac{\partial N_{xy}}{\partial x} + \frac{\partial N_y}{\partial y} = 0 \\ &\delta w_0: \quad \frac{\partial^2 M_x^b}{\partial x^2} + 2\frac{\partial^2 M_{xy}^b}{\partial x\partial y} + \frac{\partial^2 M_y^b}{\partial y^2} + q - R = 0 \\ &\delta\theta: \quad -\mathrm{N}_z - k_1 M_x^s - k_2 M_y^s - (k_1 A' + k_2 B')\frac{\partial^2 M_{xy}^s}{\partial x\partial y} \\ &+k_1 A'\frac{\partial Q_{xz}^s}{\partial x} + k_2 B'\frac{\partial Q_{yz}^s}{\partial y} + \frac{\partial S_{xz}^s}{\partial x} + \frac{\partial S_{yz}^s}{\partial y} + qg(z) - Rg(z) = 0\end{aligned} \tag{24}$$

The stress resultants are obtained as:

$$\begin{Bmatrix} N \\ M^b \\ M^s \end{Bmatrix} = \begin{bmatrix} A & B & B^s \\ B & D & D^s \\ B^s & D^s & H^s \end{bmatrix} \begin{Bmatrix} \varepsilon \\ k^b \\ k^s \end{Bmatrix} + \begin{bmatrix} L \\ L^a \\ R \end{bmatrix} \varepsilon_0^z \tag{25a}$$

$$\begin{Bmatrix} Q \\ S \end{Bmatrix} = \begin{bmatrix} F^s & X^s \\ X^s & A^s \end{bmatrix} \begin{Bmatrix} \gamma^0 \\ \gamma^1 \end{Bmatrix}$$

$$N_z = R^a\varepsilon_z^0 + L(\varepsilon_x^0 + \varepsilon_y^0) + L^a(k_x^b + k_y^b) + R(k_x^s + k_y^s) \tag{25b}$$

where

$$\begin{aligned}N = \{N_x, N_y, N_{xy}\},\; M^b = \{M_x^b, M_y^b, M_{xy}^b\}, \\ M^s = \{M_x^s, M_y^s, M_{xy}^s\}\end{aligned} \tag{26a}$$

$$S = \{S_{xz}^s, S_{yz}^s\},\; Q = \{Q_{xz}^s, Q_{yz}^s\}, \tag{26b}$$

$$\gamma^0 = \{\gamma_{xz}^0, \gamma_{yz}^0\},\; \gamma^1 = \{\gamma_{xz}^1, \gamma_{yz}^1\}, \tag{26c}$$

$$\varepsilon = \{\varepsilon_x^0, \varepsilon_y^0, \varepsilon_{xy}^0\},\; k^b = \{k_x^b, k_y^b, k_{xy}^b\},\; k^s = \{k_x^s, k_y^s, k_{xy}^s\} \tag{26d}$$

$$\begin{aligned}A = \begin{bmatrix} A_{11} & A_{12} & 0 \\ A_{12} & A_{22} & 0 \\ 0 & 0 & A_{66} \end{bmatrix},\; B = \begin{bmatrix} B_{11} & B_{12} & 0 \\ B_{12} & B_{22} & 0 \\ 0 & 0 & B_{66} \end{bmatrix}, \\ D = \begin{bmatrix} D_{11} & D_{12} & 0 \\ D_{12} & D_{22} & 0 \\ 0 & 0 & D_{66} \end{bmatrix}\end{aligned} \tag{26e}$$

$$\begin{aligned}B^s = \begin{bmatrix} B_{11}^s & B_{12}^s & 0 \\ B_{12}^s & B_{22}^s & 0 \\ 0 & 0 & B_{66}^s \end{bmatrix},\; \mathrm{D}^s = \begin{bmatrix} D_{11}^s & D_{12}^s & 0 \\ D_{12}^s & D_{22}^s & 0 \\ 0 & 0 & D_{66}^s \end{bmatrix}, \\ \mathrm{H}^s = \begin{bmatrix} H_{11}^s & H_{12}^s & 0 \\ H_{12}^s & H_{22}^s & 0 \\ 0 & 0 & H_{66}^s \end{bmatrix}\end{aligned} \tag{26f}$$

$$\begin{Bmatrix} L \\ L^a \\ R \\ R^a \end{Bmatrix} = \int_{-h/2}^{h/2} \lambda(z,T) \begin{Bmatrix} 1 \\ z \\ f(z) \\ g'(z)\dfrac{1-\nu}{\nu} \end{Bmatrix} g'(z)dz \tag{26f}$$

and stiffness components are given as:

$$\begin{Bmatrix} A_{11} & B_{11} & D_{11} & B_{11}^s & D_{11}^s & H_{11}^s \\ A_{12} & B_{12} & D_{12} & B_{12}^s & D_{12}^s & H_{12}^s \\ A_{66} & B_{66} & D_{66} & B_{66}^s & D_{66}^s & H_{66}^s \end{Bmatrix} =$$

$$\int_{-h/2}^{h/2} \lambda(z,T)\left[1,\ z,\ z^2,\ f(z),\ zf(z),\ f^2(z)\right] \begin{Bmatrix} \dfrac{1-\nu}{\nu} \\ 1 \\ \dfrac{1-2\nu}{2\nu} \end{Bmatrix} dz \tag{27a}$$

$$F^s = \begin{bmatrix} F_{44}^s & 0 \\ 0 & F_{55}^s \end{bmatrix}, A^s = \begin{bmatrix} A_{44}^s & 0 \\ 0 & A_{55}^s \end{bmatrix}, X^s = \begin{bmatrix} X_{44}^s & 0 \\ 0 & X_{55}^s \end{bmatrix} \tag{27b}$$

$$(F_{44}^s, X_{44}^s, A_{44}^s) = (F_{55}^s, X_{55}^s, A_{55}^s) = \int_{-h/2}^{h/2} \left(\frac{E(z,T)}{2(1+\nu)}\right) [f'?z), f'(z)g(z), g?z)])\, dz \tag{27c}$$

$$(A_{22},\ B_{22},\ D_{22},\ B_{22}^s,\ D_{22}^s,\ H_{22}^s) = (A_{11},\ B_{11},\ D_{11},\ B_{11}^s,\ D_{11}^s,\ H_{11}^s) \tag{27d}$$

By substituting Eq. (25) into Eq. (24), the equation of motion can be expressed in terms of displacements (u_0, v_0, w_0, θ) and the appropriate equations take the form:

$$\begin{aligned} &\delta u_0 : A_{11}\frac{\partial^2 u_0}{\partial x^2} + A_{12}\frac{\partial^2 v_0}{\partial x \partial y} + A_{66}\left(\frac{\partial^2 u_0}{\partial y^2} + \frac{\partial^2 v_0}{\partial x \partial y}\right) - B_{11}\frac{\partial^3 w_0}{\partial x^3} \\ &-B_{12}\frac{\partial^3 w_0}{\partial x \partial y^2} - 2B_{66}\frac{\partial^3 w_0}{\partial x \partial y^2} + (B_{11}^s k_1 + B_{12}^s k_2 + L)\frac{\partial \theta}{\partial x} \\ &+B_{66}^s\left(A'k_1 + B'k_2\right)\frac{\partial^3 \theta}{\partial x \partial y^2} = 0 \end{aligned} \tag{28a}$$

$$\begin{aligned} &\delta v_0 : A_{12}\frac{\partial^2 u_0}{\partial x \partial y} + A_{22}\frac{\partial^2 v_0}{\partial y^2} + A_{66}\left(\frac{\partial^2 u_0}{\partial x \partial y} + \frac{\partial^2 v_0}{\partial x^2}\right) - B_{12}\frac{\partial^3 w_0}{\partial x^2 \partial y} \\ &-B_{22}\frac{\partial^3 w_0}{\partial y^3} - 2B_{66}\frac{\partial^3 w_0}{\partial x^2 \partial y} + (B_{12}^s k_1 + B_{22}^s k_2 + L)\frac{\partial \theta}{\partial y} \\ &+B_{66}^s\left(A'k_1 + B'k_2\right)\frac{\partial^3 \theta}{\partial x^2 \partial y} = 0 \end{aligned} \tag{28b}$$

$$\begin{aligned} &\delta w_0 : B_{11}\frac{\partial^3 u_0}{\partial x^3} + (B_{12} + 2B_{66})\frac{\partial^3 u_0}{\partial x \partial y^2} + (B_{12} + 2B_{66})\frac{\partial^3 v_0}{\partial x^2 \partial y} \\ &+B_{22}\frac{\partial^3 v_0}{\partial y^3} - D_{11}\frac{\partial^4 w_0}{\partial x^4} - (2D_{12} + 4D_{66})\frac{\partial^4 w_0}{\partial x^2 \partial y^2} - D_{22}\frac{\partial^4 w_0}{\partial y^4} \\ &+(D_{12}^s k_2 + D_{11}^s k_1 + L^a)\frac{\partial^2 \theta}{\partial x^2} + (D_{12}^s k_1 + D_{22}^s k_2 + L^a)\frac{\partial^2 \theta}{\partial y^2} + \\ &2D_{66}^s(A'k_1 + B'k_2)\frac{\partial^4 \theta}{\partial x^2 \partial y^2} + q - R = 0 \end{aligned} \tag{28c}$$

$$\begin{aligned} &\delta\theta : -(L + k_1 B_{11}^s + k_2 B_{12}^s)\frac{\partial u_0}{\partial x} - (A'k_1 + B'k_2)B_{66}^s\frac{\partial^3 u_0}{\partial x^1 \partial y^2} \\ &-(L + k_1 B_{12}^s + k_2 B_{22}^s)\frac{\partial v_0}{\partial y} - (A'k_1 + B'k_2)B_{66}^s\frac{\partial^3 v_0}{\partial x^2 \partial y^1} \\ &+(L^a + k_1 D_{11}^s + k_2 D_{12}^s)\frac{\partial^2 w_0}{\partial x^2} + (L^a + k_1 D_{12}^s + k_2 D_{22}^s)\frac{\partial^2 w_0}{\partial y^2} + \\ &2(A'k_1 + B'k_2)D_{66}^s\frac{\partial^4 w_0}{\partial x^2 \partial y^2} - (k_1{}^2 H_{11}^s + 2k_1 R + 2k_1 k_2 H_{12}^s \\ &+k_2{}^2 H_{22}^s + 2Rk_2 + R^a)\theta + (k_2{}^2 B'^2 F_{44}^s + k_2 B' X_{44}^s)\frac{\partial^2 \theta}{\partial y^2} \\ &+(A_{44}^s + k_2 B' X_{44}^s)\frac{\partial^2 \theta}{\partial y^2} + (k_1{}^2 A'^2 F_{44}^s + k_1 A' X_{44}^s)\frac{\partial^2 \theta}{\partial x^2} + \\ &(A_{44}^s + k_1 A' X_{44}^s)\frac{\partial^2 \theta}{\partial x^2} - H_{66}^s(A'k_1 + B'k_2)^2\frac{\partial^4 \theta}{\partial x^2 \partial y^2} \\ &+qg(z) - Rg(z) = 0 \end{aligned} \tag{28d}$$

3.4 Temperature field

Thermal analysis is performed by imposing constant surface temperatures on ceramic and metal-rich surfaces. The temperature variation is assumed to occur only in the thickness direction. The thermal analysis is conducted by solving the one-dimensional heat conduction equation. The one dimensional steady-state heat conduction equation in the z-direction is given by:

$$-\frac{d}{dz}\left(k(z)\frac{dT}{dz}\right) = 0 \tag{29}$$

With the boundary condition T(h/2) = T_t and T(−h/2)=T_b=T_0. Here a stress-free state is assumed to exist at T_0=300 K. The analytical solution of the Eq. (29) is:

$$T(z) = T_b - (T_t - T_b)\frac{\int_{-h/2}^{z} \frac{1}{k(z)}dz}{\int_{-h/2}^{h/2} \frac{1}{k(z)}dz} \tag{30}$$

In the case of power-law FG plate, the solution of Eq. (29) also can be expressed by means of a polynomial series as:

$$T(z) = T_b + \frac{(T_t - T_b)}{C_{tb}}\begin{bmatrix} \left(\dfrac{2z+h}{2h}\right) - \dfrac{k_{tb}}{(p+1)k_b}\left(\dfrac{2z+h}{2h}\right)^{p+1} \\ +\dfrac{k_{tb}^2}{(2p+1)k_b^2}\left(\dfrac{2z+h}{2h}\right)^{2p+1} \\ -\dfrac{k_{tb}^3}{(3p+1)k_b^3}\left(\dfrac{2z+h}{2h}\right)^{3p+1} \\ +\dfrac{k_{tb}^4}{(4p+1)k_b^4}\left(\dfrac{2z+h}{2h}\right)^{4p+1} \\ -\dfrac{k_{tb}^5}{(5p+1)k_b^5}\left(\dfrac{2z+h}{2h}\right)^{5p+1} \end{bmatrix} \tag{31}$$

with

$$C_{tb}=\left[\begin{array}{l}1-\dfrac{k_{tb}}{(p+1)k_b}+\dfrac{k_{tb}^2}{(2p+1)k_b^2}-\dfrac{k_{tb}^3}{(3p+1)k_b^3}\\ +\dfrac{k_{tb}^4}{(4p+1)k_b^4}-\dfrac{k_{tb}^5}{(5p+1)k_b^5}\end{array}\right] \tag{32}$$

where $k_{tb}=k_t-k_b$, with k_t and k_b are the thermal conductivity of the top and bottom faces of the plate, respectively.

4. Close form solution for simply supported FG Plate

Rectangular plates are generally classified according to the type of support used. This paper is concerned with the exact solutions of Eqs. (28a)-(28d) for a simply supported FG plate. The following boundary conditions are imposed at the edges:

$$\begin{aligned} v_0=w_0=\theta=\frac{\partial\theta}{\partial y}=\varphi=N_x=M_x^b=M_x^s=0 \qquad \text{at } x=0,a\\ u_0=w_0=\theta=\frac{\partial\theta}{\partial x}=\varphi=N_y=M_y^b=M_y^s=0 \qquad \text{at } y=0,b\end{aligned} \tag{33}$$

Following the Navier solution procedure, the authors assume the following solution from for $\boldsymbol{u_0}$, $\boldsymbol{v_0}$, $\boldsymbol{w_0}$, and $\boldsymbol{\theta}$ that satisfies the boundary conditions given in:

$$\left\{\begin{array}{l}u_0\\ v_0\\ w_0\\ \theta\end{array}\right\}=\left\{\begin{array}{l}U_{mn}\cos(\lambda x)\sin(\mu y)\\ V_{mn}\sin(\lambda x)\cos(\mu y)\\ W_{mn}\sin(\lambda x)\sin(\mu y)\\ X_{mn}\sin(\lambda x)\sin(\mu y)\end{array}\right\} \tag{34}$$

where U_{mn}, V_{mn}, W_{mn} and X_{mn} and are arbitrary parameters to be determined and λ, μ are defined as:

$$\alpha=m\pi/a \quad \text{and} \quad \beta=n\pi/b \tag{35}$$

The transverse load q is also expanded in the double-Fourier sine series as

$$q(x,y)=\sum_{m=1}^{\infty}\sum_{n=1}^{\infty}q_{mn}\sin(\alpha x)\sin(\beta y) \tag{36}$$

The analytical solutions can be obtained from:

$$\left[\begin{array}{llll}a_{11}&a_{12}&a_{13}&a_{14}\\ a_{12}&a_{22}&a_{23}&a_{24}\\ a_{13}&a_{23}&a_{33}&a_{34}\\ a_{14}&a_{24}&a_{34}&a_{44}\end{array}\right]\left\{\begin{array}{l}U_{mn}\\ V_{mn}\\ W_{mn}\\ X_{mn}\end{array}\right\}=\left\{\begin{array}{l}0\\ 0\\ q_{mn}\\ 0\end{array}\right\} \tag{37}$$

in which:

$$\begin{aligned} a_{11}&=(A_{11}\alpha^2+A_{66}\beta^2)\\ a_{12}&=\alpha\beta\left(A_{12}+A_{66}\right)\\ a_{13}&=-\alpha(B_{11}\alpha^2+(B_{12}+2B_{66})\beta^2)\\ a_{14}&=\alpha(B_{11}^sk_1)+(B_{12}^s+2B_{66}^s)\alpha\beta^2-L\alpha\\ a_{22}&=\alpha^2A_{66}+\beta^2A_{22}\\ a_{23}&=-\beta(B_{22}\beta^2+(B_{12}+2B_{66})\alpha^2)\end{aligned} \tag{38}$$

$$\begin{aligned} a_{23}&=-\beta(B_{22}\beta^2+(B_{12}+2B_{66})\alpha^2)\\ a_{24}&=\beta B_{22}^sk_2+(B_{12}^s+2B_{66}^s)\alpha^2\beta-L\beta\\ a_{33}&=\alpha^2\left(D_{11}\alpha^2+\left(2D_{12}+4D_{66}\right)\beta^2\right)+D_{22}\beta^4\\ &\quad+\overline{K}+\overline{G}(\alpha^2+\beta^2)\\ a_{34}&=-D_{11}^sk_1\alpha^2-D_{12}^s\left(\alpha^2k_2+\beta^2k_1\right)-D_{22}^sk_2\beta^2\\ &\quad+2D_{66}^s\left(A'k_1+B'k_2\right)\beta^2\alpha^2+L_a(\beta^2+\alpha^2)\\ &\quad+g(z)\overline{K}+g(z)\overline{G}(\alpha^2+\beta^2)\end{aligned} \tag{38}$$

$$\begin{aligned} a_{44}&=H_{11}^sk_1^2+2k_1k_2(H_{12}^s+2H_{66}^s)+H_{22}^sk_2^2\\ &+\beta^2(B^2F_{44}^sk_2^2-BX_{44}^sk_2)+\alpha^2(A^2F_{44}^sk_1^2-AX_{44}^sk_1)\\ &+\beta^2(-BX_{44}^sk_2+A_{44}^s)+\alpha^2(X_{44}^s+A_{44}^s)-2(k_1+k_2)R\\ &+Ra+g?\,z)\overline{K}+g(z)?\overline{G}\,\alpha^2+\beta^2)\end{aligned}$$

5. Numerical results and discussion

In this section, thermal bending response of FG plate resting on variable elastic foundation is investigated based on a quasi 3D solution. The FG plate is subjected to thermo-mechanical loading.

This section will be divided into three parts: validation of results, parametric study and effect of micromechanical models on the response of FG plates on variable foundations.

The FGM plate is taken to be made of Titanium alloy (Ti-6Al-4V) and Zirconia (ZrO_2). Temperature-dependent coefficients of Young's modulus E, thermal expansion α and thermal conductivity k are given in Table 1. While the Poisson's ratio is assumed to be a constant υ=0.3.

The following dimensionless expressions are used in the present analysis:

$$\begin{aligned} &\overline{w}=\frac{100h}{q_0a^2}w\left(\frac{a}{2},\frac{b}{2}\right), \quad \overline{\sigma_x}=-\frac{10h^2}{q_0a^2}\sigma_x\left(\frac{a}{2},\frac{b}{2},\frac{h}{2}\right),\\ &\overline{\tau_{xz}}=-\frac{10hb}{q_0a^2}\tau_{xz}\left(0,\frac{b}{2},0\right) \quad \overline{\tau_{xy}}=-\frac{100h^2b}{q_0a^3}\tau_{xy}\left(0,0,-\frac{h}{2}\right),\\ &\overline{\tau_{yz}}=-\frac{10h}{q_0a}\tau_{yz}\left(\frac{a}{2},0,z\right), \quad J_2=\frac{\overline{G}a^2}{h^3}\end{aligned}$$

Table 1 Material properties used in the FG plate

	P_0	P_{-1}	P_1	P_2	P_3
			ZrO2 (Ceramic)		
E	244.27 e^{+9}	0	-1.371 e^{-3}	1.214 e^{-6}	–3.681e^{-10}
α	12.766 e^{-6}	0	-1.491 e^{-3}	1.006 e^{-5}	–6.778e^{-11}
k	1.8	0	0	0	0
υ	0.3	0	0	0	0
			Ti–4V–6Al (Metal)		
E	122.56e^{+9}	0	-4.586e^{-4}	0	0
α	7.5788e^{-6}	0	6.638e^{-4}	–3.147e^{-6}	0
k	7.82	0	0	0	0
υ	0.3	0	0	0	0

Table 2 The deflection $\bar{w}$ of FGM square and rectangular plate simply supported and resting on elastic foundations (ΔT=300, p=1)

m	n	Theory	Square plate	Rectangular plate (b/a=2)
1	1	SPT – Sobhy (2015) 2D	1.57312	3.11472
		Attia *et al.* (2018) 2D	1.58118	3.14664
		Present 3D	1.58019	3.14943
	3	SPT - Sobhy (2015) 2D	-0.10770	-0.72382
		Attia *et al.* (2018) 2D	-0.10770	-0.72551
		Present 3D	-0.10578	-0.72290
2	1	SPT - Sobhy (2015) 2D	0.00000	0.00000
		Attia *et al.* (2018) 2D	0.00000	0.00000
		Present 3D	0.00000	0.00000
	3	SPT - Sobhy (2015) 2D	0.00000	0.00000
		Attia *et al.* (2018) 2D	0.00000	0.00000
		Present 3D	0.00000	0.00000
3	1	SPT - Sobhy (2015) 2D	-0.10765	-0.12701
		Attia *et al.* 2018	-0.10773	-0.12296
		Present 3D	-0.10578	-0.12091
	3	SPT - Sobhy (2015) 2D	0.04059	0.08825
		Attia *et al.* (2018) 2D	0.04060	0.08831
		Present 3D	0.03936	0.08651
4	1	SPT - Sobhy (2015) 2D	0.00000	0.00000
		Attia *et al.* (2018) 2D	0.00000	0.00000
		Present 3D	0.00000	0.00000
	3	SPT - Sobhy (2015) 2D	0.00000	0.00000
		Attia *et al.* (2018) 2D	0.00000	0.00000
		Present 3D	0.00000	0.00000

Table 3 The deflection $\bar{w}$ of FGM square plates without or resting on elastic foundations (ΔT=300, p=1, ξ=0)

J1	J2	Theory	a/h						
			5	10	15	20	25	30	50
0	0	FPT - Sobhy (2015) 2D	0.72464	2.50034	5.45984	9.60314	14.93025	21.44115	59.32280
		HPT - Sobhy (2015) 2D	0.72413	2.50010	5.45965	9.60296	14.93007	21.44098	59.32257
		SPT - Sobhy (2015) 2D	0.72385	2.49988	5.45944	9.60276	14.92988	21.44079	59.32241
		Attia *et al.* (2018) 2D	0.72382	2.49972	5.45916	9.60237	14.92936	21.44014	59.32124
		Present 3D	0.70872	2.48344	5.44116	9.58200	14.90590	21.41292	59.27192
10^3	0	FPT - Sobhy (2015) 2D	0.56180	2.00022	4.39367	7.74398	12.05137	17.31589	47.94570
		HPT - Sobhy (2015) 2D	0.56149	2.00006	4.39355	7.74386	12.05126	17.31578	47.94558
		SPT - Sobhy (2015) 2D	0.56132	1.99992	4.39367	7.74373	12.05113	17.31566	47.94544
		Attia *et al.* (2018) 2D	0.56130	1.99982	4.39323	7.74347	12.0508	17.31526	47.94468
		Present 3D	0.55604	1.99318	4.38539	7.73404	12.03934	17.30132	47.91632
10^3	10^3	FPT - Sobhy (2015) 2D	0.10335	0.40422	0.90506	1.60613	2.50748	3.60913	10.01867
		HPT - Sobhy (2015) 2D	0.10334	0.40421	0.90505	1.60612	2.50748	3.60912	10.01865
		SPT - Sobhy (2015) 2D	0.10333	0.40421	0.90505	1.60612	2.50747	3.60912	10.01865
		Attia *et al.* (2018) 2D	0.10333	0.40420	0.90504	1.60612	2.50746	3.60910	10.01862
		Present 3D	0.10586	0.40704	0.90793	1.60897	2.51026	3.61180	10.02070

Table 4 The transverse shear stress $\overline{\tau_{xz}}$ in FGM square plates with or without elastic foundations (ΔT=300, p=1, $\xi = 0$)

J1	J2	Theory	a/h						
			5	10	15	20	25	30	50
0	0	FPT - Sobhy (2015) 2D	1.91547	1.91547	1.91547	1.91547	1.91547	1.91547	1.91547
		HPT - Sobhy (2015) 2D	2.38438	2.38915	2.39004	2.39035	2.39049	2.39057	2.39069
		SPT - Sobhy (2015) 2D	2.45911	2.46518	2.46632	2.46671	2.46687	2.46700	2.46714
		Attia *et al.* (2018) 2D	2.45911	2.46517	2.46630	2.46669	2.46683	2.46698	2.46713
		Present 3D	2.24585	2.40065	2.45867	2.48368	2.49631	2.50348	2.51432
10^3	0	FPT - Sobhy (2015) 2D	1.48501	1.53232	1.54142	1.54462	1.54612	1.54694	1.54811
		HPT - Sobhy (2015) 2D	1.84885	1.91131	1.92334	1.92758	1.92956	1.93062	1.93220
		SPT - Sobhy (2015) 2D	1.90696	1.97216	1.98473	1.98918	1.99122	1.99235	1.99399
		Attia *et al.* (2018) 2D	1.90698	1.97219	1.98474	1.98918	1.99124	1.99236	1.99398
		Present 3D	1.76200	1.92674	1.98160	2.00469	2.01624	2.02278	2.03261
10^3	10^3	FPT - Sobhy (2015) 2D	0.27321	0.30969	0.31754	0.32037	0.32171	0.32243	0.32349
		HPT - Sobhy (2015) 2D	0.34029	0.38629	0.39624	0.39981	0.40149	0.40245	0.40379
		SPT - Sobhy (2015) 2D	0.35107	0.39860	0.40886	0.41257	0.41433	0.41525	0.41667
		Attia *et al.* (2018) 2D	0.35107	0.39862	0.40887	0.41258	0.41432	0.41527	0.41666
		Present 3D	0.33545	0.39347	0.41026	0.41705	0.42039	0.42227	0.42507

Unless otherwise specified the following values will be used: a/h=10, J_1=J_2=100, b/a=1, m=n=1, q_0=10^5, ξ=10.

It is also recalled that the Voigt model is used in the different calculations unless otherwise indicated.

5.1 Validation of results

First, numerical tests are performed to confirm the accuracy of the proposed model. For verification purpose, the obtained results are compared with those of the 2D solutions of Attia *et al.* (2018) and Sobhy (2015).

Table 2 examines the non-dimensional central deflection in terms of mod numbers (m,n) for FG plate type ZrO2/Ti–6Al–4V resting on elastic foundations with a parabolic Winkler modulus. It can be seen from this results, that there is a good agreement between our findings for the thermal bending of FGM plates and the findings of Attia *et al.* (2018) and Sobhy (2015) and this for both cases of rectangular and square plate.

Another example is performed in table 3 for a FG plate with or without elastic foundation for different values of the side-to-thickness ratio a/h. The results of the non-dimensional central deflection for the present method are compared with those of Sobhy (2015) for different HSDT theories and those of Attia *et al.* (2018). The comparison shows that there is a good agreement. The small difference that exists is that the present theory is 3D and that by its nature takes into account the stretching effect in its formulation. This effect is neglected in the other 2D theories.

Table 4 shows a further comparison of the results of the present formulation with those of the literature. The variation of the shear stresses $\overline{\tau_{xz}}$ as a function of the a/h ratio for different configurations of the FG plate with or without elastic foundation is exposed.

There is good agreement between our results and those of Sobhy (2015) (HPT and SPT) and Attia *et al.* (2018). The slight difference that exists for small a/h values where the plate is considered to be thick can be explained by the fact that HSDTs neglect the effect of stretching thing that is taken into consideration by the present 3D solution.

This difference becomes less important when a/h increases i.e., when we tend towards thin plates. Regarding the difference that exists with Sobhy's SPT (2015), the latter requires a shear correction factor and the distribution of shear stresses is not as accurate as the others.

After these comparisons, it can be concluded that the present quasi 3D solution with only four unknowns is not only accurate but also efficient in predicting the thermo-mechanical responses of FG plates resting on elastic foundation.

5.2 Parametric study

After confirming the validity of the current theory and formulation, some results are exposed to show the effects of the power law index, elastic foundation, plate geometry, and temperature field on the thermal bending of FG plates.

Fig. 2(a) and 2(b) displays the variation of deflection $\bar{w}$ versus the side-to-thickness ratio a/h for different power law index for FG plate resting on parabolic elastic foundations.

Two cases are studied: FG plate under mechanical loading and thermo-mechanical loading. It is noted that deflection $\bar{w}$ increases as the ratio a/h increases whatever the loading applied and the type of plate (isotropic or FG).

Also, the deflection of the FG plate is between those of the two isotropic plates (rich metal and rich ceramic).

The variations of transverse shear stress $\overline{\tau_{xz}}$ through the thickness of FG plate resting on parabolic elastic

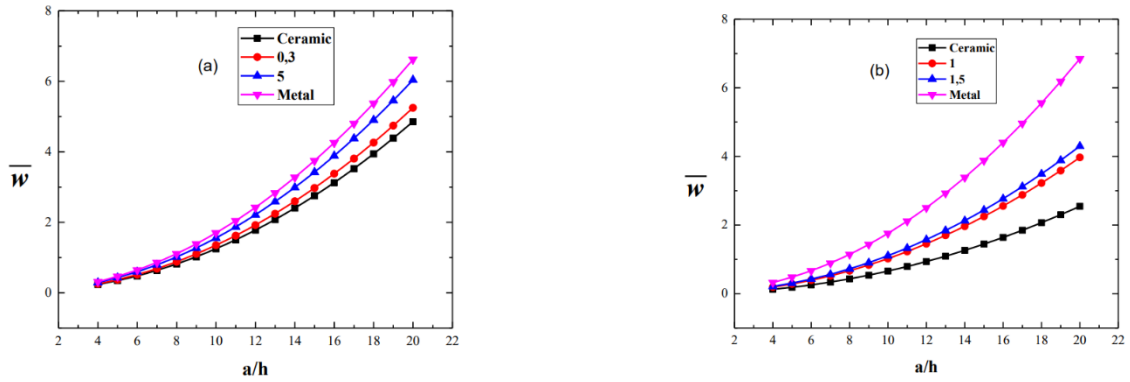

Fig. 2 Variation of deflection $\overline{w}$ versus the side-to-thickness ratio *a/h* for different power law index. (a) FG plate under mechanical loading and (b) FG plate under thermo-mechanical loading

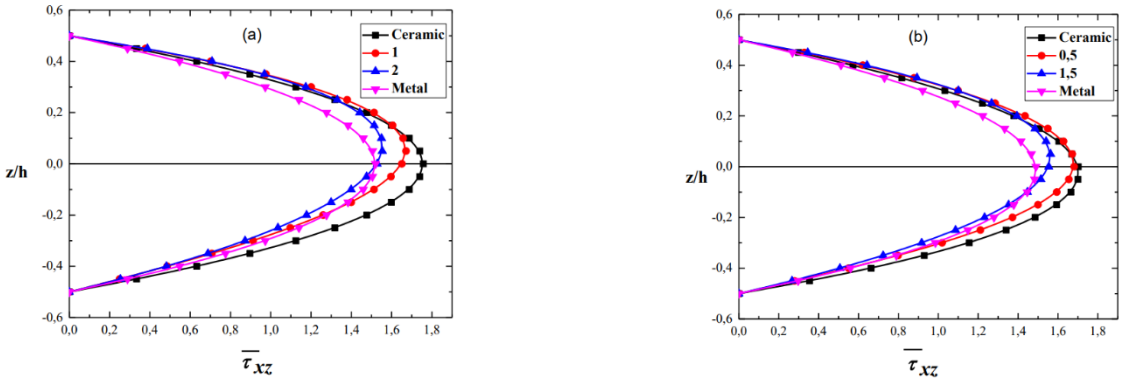

Fig. 3 Variation of transverse shear stress $\overline{\tau_{xz}}$ through the thickness of FG plate for different power law index. (a) FG plate under mechanical loading and (b) FG plate under thermo-mechanical loading (ΔT=200)

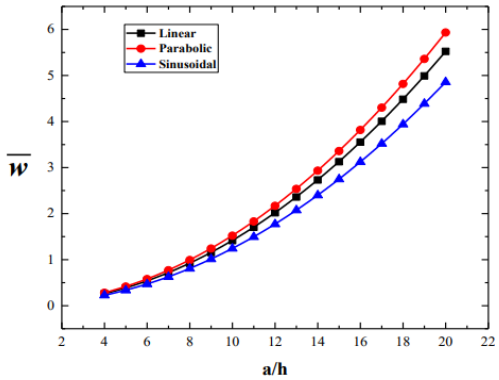

Fig. 4 The deflection $\overline{w}$ of FG plate under thermomechanical load versus the side to thickness ratio *a/h* for various types of Winkler parameter. (*p*=1, ξ =20, ΔT=300)

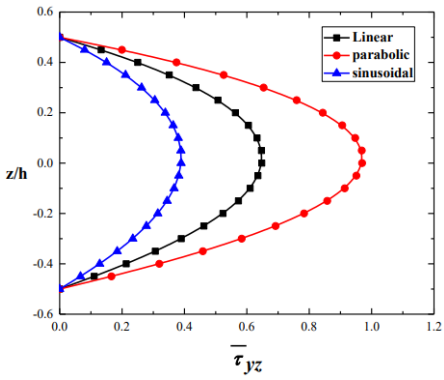

Fig. 5 Variation of transverse shear stress $\overline{\tau_{yz}}$ of FG plate under thermomechanical load versus the side to thickness ratio *a/h* for various types of Winkler parameter. (*p*=1, ξ =20, ΔT=300)

foundations for different power law index are shown graphically in Fig. 3.

The results indicate that for the case of isotropic plate, the maximum of the shear stress appears in the center of the plate which is not the case for FG plates. This is obvious since that FG plate is heterogeneous. Also, the max of these stress decreases by increasing the values of the power index.

Figs. 4 and 5 show respectively the variation of the deflection $\overline{w}$ and shear stress $\overline{\tau_{yz}}$ of FG plates under thermomechanical loading versus the side to thickness ratio a/h for the three cases of the Winkler parameter linear, parabolic and sinusoidal. The results reveal that the shear stresses are very strongly influenced by the Winkler parameter compared to the deflections.

Fig. 6 plots the variation of the deflection $\overline{w}$ of FG plate under thermomechanical loading versus the side to thickness ratio *a/h* for different values of the parabolic parameter ξ.

The figure shows that increasing this parameter reduces

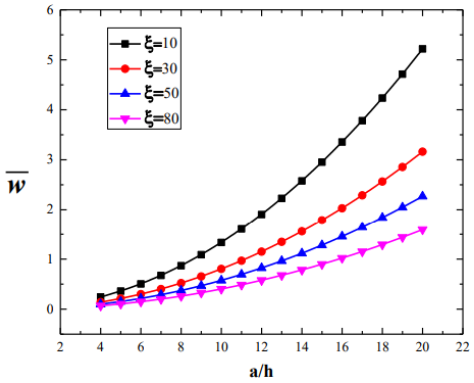

Fig. 6 Variation of the deflection $\overline{w}$ of FG plate versus the side to thickness ratio *a/h* under thermomechanical loading for different values of the parabolic parameter ξ (J_1 =1000,ΔT=300, p =1)

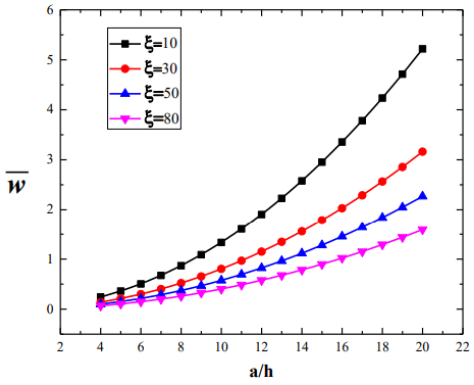

Fig. 7 The deflection $\overline{w}$ of the FGM plate against the power law index p for different micromechanical models resting on parabolic elastic foundations (ξ=10, J_1=J_2=100, ΔT=0)

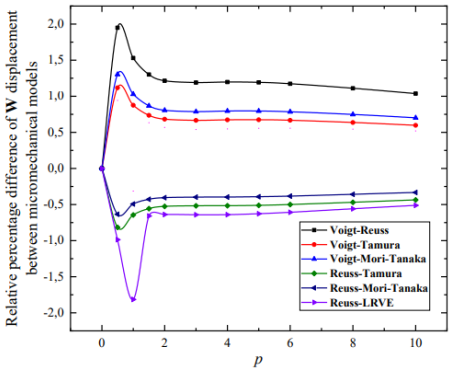

Fig. 8 Relative percentage difference between the micromechanical models of deflection $\overline{w}$ of the FG plate

the deflection. This can be explained by the fact that increasing this parameter increases the rigidity of the plate.

5.3 Effect of the micromechanical models

Most of the research in the literature employs the Voigt micromechanical scheme for multiscale simulation of the mechanical behavior of FG components. The aim of this parametric study is to discuss the influence of the micromechanical rules on the thermo-mechanical behavior

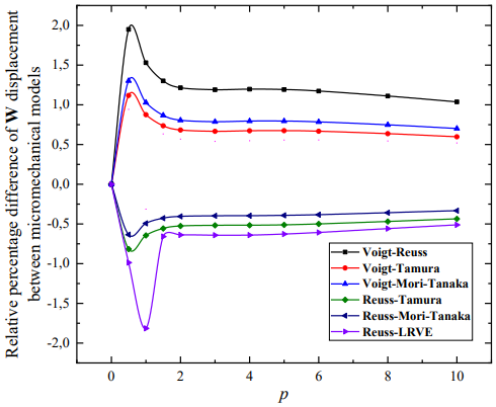

Fig. 9 Variation of the transverse shear stress $\overline{\tau_{xz}}$ through the thickness of FG plate for different micromechanical models resting on parabolic elastic foundations (p=1, ξ=10, J_1=J_2=100, ΔT=0)

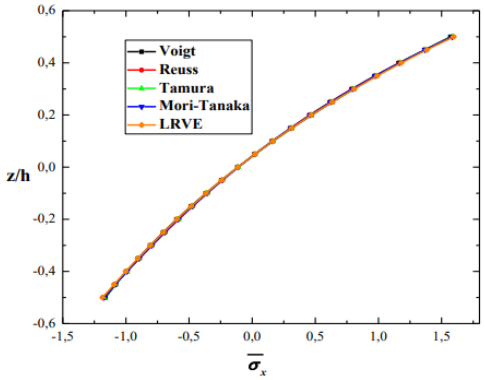

Fig. 10 Variation of in plane longitudinal stress $\overline{\sigma_x}$ through the thickness of FG plate for different micromechanical models resting on parabolic elastic foundations (p=1, ξ=10, J_1=J_2=100, ΔT=0)

of FG plate resting on variable foundation.

In Fig. 7, the variations of the deflection of FG plate resting on parabolic elastic foundation with the power law index p are given for different micromechanical models.

It is seen from the figure that the increase of the power law index p produces a raise of the deflection values. In addition, all models give the same deflection value for the case of an isotropic plate (p = 0). The difference between the different models in terms of deflection increases imperceptibly with the increase in the power index values. The highest values are obtained by the Reuss model and the lowest by Voigt. The other models are in between the two above. However, the differences between the different models remain small.

Relative Percentage difference of the deflection between micromechanical models versus power law index p is shown in Fig. 8. The discrepancy between the estimated deflection of FGMs by the Voigt, Reuss and other micromechanical models is not heavily dependent on the power law index p. The discrepancy between the Voigt model and other micro-mechanical models for the estimated values of the deflection reaches a maximum of 2% between Voigt and Reuss and it is 1,3% between Voigt and Mori-Tanaka. While between Voigt and other model namely

Tamura it does not exceed 1,15 %.

The second comparison shown in this figure is the discrepancy between the values of deflection between the Reuss model and other micromechanical models. The difference is insignificant between Reuss and Mori-Tanaka and it reached a maximum of 1,8 % between Reuss and LRVE. It should be noted that these differences max between micro-mechanical models are obtained for a value of $p = 1$. Exceeding the value of $p = 2$, all models keep a more or less constant difference not exceeding 1%.

Fig. 9 shows the variation of the transverse shear stress for different micromechanical models through the thickness of FG plate resting on parabolic elastic foundation. The maximum values of the stress are obtained by the Voigt model and the lowest by the LRVE model. The other models give values between the first two.

Fig. 10 plots the variation of the in plane longitudinal stress for different micromechanical models through the thickness. As can be seen from this figure, all micromechanical models give the same values stress.

In overall, it is clear that the use of one micromechanical model or another for the determination of the effective properties of an FG plate resting on variable elastic foundation supporting a thermo-mechanical load does not strongly affect the response of this plate in terms of displacements and stress.

6. Conclusions

This paper has studied the behavior of temperature-dependent FG plates resting on variable elastic foundation and being exposed to thermomechanical loading, based on a quasi 3D theory. Several micromechanical models have been employed to obtain the effective material properties of the FG plate. The governing equations have been solved by the Navier method for stability analysis of simply supported FG plates. The current study is compared to existing numerical results where a good agreement has been found. A detailed parametric study is presented to highlight the effects of all parameters influencing the thermomechanical behavior of FG plates resting on an elastic foundation. It was also found that the difference between the micromechanical models does not affect the response in terms of displacement and stress of FG plate on elastic foundation. Other works can be carried out in future by considering other types of materials and other models with shear deformation effect (Salamat and Sedighi 2017, Panjehpour *et al.* 2018, Othman and Fekry 2018, Fenjan *et al.* 2019b, Bohlooly and Fard 2019, Hamad *et al.* 2019, Medani *et al.* 2019, Selmi 2019, Alimirzaei *et al.* 2019, Al-Maliki *et al.* 2019, Nikkhoo *et al.* 2019, Kossakowski and Uzarska 2019, Hussain *et al.* 2019 and 2020a, b, Semmah *et al.* 2019, Fládr *et al.* 2019, Bakhshi and Taheri-Behrooz 2019, Karami *et al.* 2019a, b, Al-Basyouni *et al.* 2020, Bellal *et al.* 2020, Ouakad *et al.* 2020, Ghadimi 2020, Ghannadpour and Mehrparvar 2020, Matouk *et al.* 2020, Taj *et al.* 2020, Bousahla *et al.* 2020, Asghar *et al.* 2020, Bourada *et al.* 2020, Timesli 2020, Lee *et al.* 2020, Shokrieh and Kondori 2020, Kar and Panda 2020).

Acknowledgments

Authors would like to acknowledge the support provided by the Directorate General for Scientific Research and Technological Development (DGRSDT).

References

Abualnour, M., Chikh, A., Hebali, H., Kaci, A., Tounsi, A., Bousahla, A.A. and Tounsi, A. (2019), "Thermomechanical analysis of antisymmetric laminated reinforced composite plates using a new four variable trigonometric refined plate theory", *Comput. Concrete*, **24**(6), 489-498. https://doi.org/10.12989/cac.2019.24.6.489.

Achouri, F., Benyoucef, S., Bourada, F, Bachir Bouiadjra, R. and Tounsi, A. (2019), "Robust quasi 3D computational model for mechanical response of FG thick sandwich plate", *Struct. Eng. Mech.*, **70**(5), 571-589. https://doi.org/10.12989/sem.2019.70.5.571.

Ahmed, R.A., Fenjan, R.M. and Faleh, N.M. (2019), "Analyzing post-buckling behavior of continuously graded FG nanobeams with geometrical imperfections", *Geomech. Eng.*, **17**(2), 175-180. https://doi.org/10.12989/gae.2019.17.2.175.

Ahmed, R.A., Fenjan, R.M. and Faleh, N.M. (2019), "Analyzing post-buckling behavior of continuously graded FG nanobeams with geometrical imperfections", *Geomech. Eng.*, **17**(2), 175-180. https://doi.org/10.12989/gae.2019.17.2.175.

Akbarzadeh, A.H., Abedini, A. and Chen, Z.T. (2015), "Effect of micromechanical models on structural responses of functionally graded plates", *Compos. Struct.*, **119**, 598-609. http://doi.org/10.1016/ j.compstruct.2014.09.031.

Akbaş, Ş.D. (2019), "Hygro-thermal nonlinear analysis of a functionally graded beam", *J. Appl. Comput. Mech.*, **5**(2), 477-485. https://doi.org/10.22055/JACM.2018.26819.1360.

Al-Basyouni, K.S., Ghandourah, E., Mostafa, H.M. and Algarni, A. (2020), "Effect of the rotation on the thermal stress wave propagation in non-homogeneous viscoelastic body", *Geomech. Eng.*, **21**(1), 1-9. https://doi.org/10.12989/gae.2020.21.1.001.

Al-Maliki, A.F., Faleh, N.M. and Alasadi, A.A. (2019), "Finite element formulation and vibration of nonlocal refined metal foam beams with symmetric and non-symmetric porosities", *Struct. Monit. Maint.*, **6**(2), 147-159. https://doi.org/10.12989/smm.2019.6.2.147.

Al-Maliki, A.F.H., Ahmed, R.A., Moustafa, N.M. and Faleh, N.M. (2020), "Finite element based modeling and thermal dynamic analysis of functionally graded graphene reinforced beams", *Adv. Comput. Des.*, **5**(2), 177-193. https://doi.org/10.12989/acd.2020.5.2.177.

Al-Maliki, A.F.H., Ahmed, R.A., Moustafa, N.M. and Faleh, N.M. (2020), "Finite element based modeling and thermal dynamic analysis of functionally graded graphene reinforced beams", *Adv. Comput. Des.*, **5**(2), 177-193. https://doi.org/10.12989/acd.2020.5.2.177.

Alimirzaei, S., Mohammadimehr, M. and Tounsi, A. (2019), "Nonlinear analysis of viscoelastic micro-composite beam with geometrical imperfection using FEM: MSGT electro-magneto-elastic bending, buckling and vibration solutions", *Struct. Eng. Mech.*, **71**(5), 485-502. https://doi.org/10.12989/sem.2019.71.5.485.

Almitani, K.H. (2018), "Buckling behaviors of symmetric and antisymmetric functionally graded beams", *J. Appl. Comput. Mech.*, **4**(2), 115-124. https://doi.org/10.22055/jacm.2017.23040.1147.

Asghar, S., Naeem, M.N., Hussain, M., Taj, M. and Tounsi, A. (2020), "Prediction and assessment of nonlocal natural

frequencies of DWCNTs: Vibration analysis", *Comput. Concrete*, **25**(2), 133-144. https://doi.org/10.12989/cac.2020.25.2.133.

Attia, A., Bousahla, A.A., Tounsi, A., Mahmoud, S.R and Alwabli, S. (2018), "A refined four variable plate theory for thermoelastic analysis of FGM plates resting on variable elastic foundation", *Struct. Eng. Mech.*, **65**(4), 453-464. https://doi.org/10.12989/sem.2018.65.4.453.

Bachir Bouiadjra, R., Mahmoudi, A., Benyoucef, S., Tounsi, A. and Bernard, F., (2018), "Analytical investigation of bending response of FGM plate using a new quasi 3D shear deformation theory: Effect of the micromechanical models", *Struct. Eng. Mech.*, **66**(3), 317-328. https://doi.org/10.12989/sem.2018.66.3.317.

Bakhshi, N. and Taheri-Behrooz, F. (2019), "Length effect on the stress concentration factor of a perforated orthotropic composite plate under in-plane loading", *Compos. Mater. Eng.*, **1**(1), 71-90. https://doi.org/10.12989/cme.2019.1.1.071.

Balubaid, M., Tounsi, A., Dakhel, B. and Mahmoud, S.R. (2019),"Free vibration investigation of FG nanoscale plate using nonlocal two variables integral refined plate theory", *Comput. Concrete*, **24**(6), 579-586. https://doi.org/10.12989/cac.2019.24.6.579.

Batou, B., Nebab, M., Bennai, R., Ait Atmane, H., Tounsi, A. and Bouremana, M. (2019), "Wave dispersion properties in imperfect sigmoid plates using various HSDTs", *Steel Compos. Struct.*, **33**(5), 699-716. https://doi.org/10.12989/scs.2019.33.5.699.

Belbachir, N., Bourada, M., Draiche, K., Tounsi, A., Bourada, F., Bousahla, A.A. and Mahmoud, S.R. (2020), "Thermal flexural analysis of anti-symmetric cross-ply laminated plates using a four variable refined theory", *Smart Struct. Syst.*, **25**(4), 409-422. https://doi.org/10.12989/sss.2020.25.4.409.

Belbachir, N., Draich, K., Bousahla, A.A., Bourada, M., Tounsi, A. and Mohammadimehr, M. (2019), "Bending analysis of anti-symmetric cross-ply laminated plates under nonlinear thermal and mechanical loadings", *Steel Compos. Struct.*, **33**(1), 81-92. https://doi.org/10.12989/scs.2019.33.1.081.

Bellal, M., Hebali, H., Heireche, H., Bousahla, A.A., Tounsi, A., Bourada, F., Mahmoud, S.R., Adda Bedia, E.A. and Tounsi, A. (2020), "Buckling behavior of a single-layered graphene sheet resting on viscoelastic medium via nonlocal four-unknown integral model", *Steel Compos. Struct.*, **34**(5), 643-655. https://doi.org/10.12989/scs.2020.34.5.643.

Berghouti, H., Adda Bedia, E.A., Benkhedda, A. and Tounsi, A. (2019), "Vibration analysis of nonlocal porous nanobeams made of functionally graded material", *Adv. Nano Res.*, **7**(5), 351-364. https://doi.org/10.12989/anr.2019.7.5.351.

Bessaim, A., Houari, M.S.A., Bousahla, A.A., Kaci, A., Tounsi, A., and Adda Bedia, E.A. (2018), "Buckling analysis of embedded nanosize FG beams based on a refined hyperbolic shear deformation theory", *J. Appl. Comput. Mech.*, **4**(3), 140-146. https://doi.org/10.22055/JACM.2017.22996.1146.

Bohlooly, M., Fard, K.M. (2019), "Buckling and postbuckling of concentrically stiffened piezo-composite plates on elastic foundations", *J. Appl. Comput. Mech.*, **5**(1), 128-140. https://doi.org/10.22055/JACM.2018.25539.1277.

Boukhlif, Z., Bouremana, M., Bourada, F., Bousahla, A.A., Bourada, M., Tounsi, A. and Al-Osta, M.A. (2019), "A simple quasi-3D HSDT for the dynamics analysis of FG thick plate on elastic foundation", *Steel Compos. Struct.*, **31**(5), 503-516. https://doi.org/10.12989/scs.2019.31.5.503.

Boulefrakh, L., Hebali, H., Chikh, A., Bousahla, A.A., Tounsi, A. and Mahmoud, S.R. (2019), "The effect of parameters of visco-Pasternak foundation on the bending and vibration properties of a thick FG plate", *Geomech. Eng.*, **18**(2), 161-178. https://doi.org/10.12989/gae.2019.18.2.161.

Bourada, F., Bousahla, A.A., Tounsi, A., Adda Bedia, E.A., Mahmoud, S.R., Benrahou, K.H. and Tounsi, A. (2020), "Stability and dynamic analyses of SW-CNT reinforced concrete beam resting on elastic-foundation", *Comput. Concrete*, In Press.

Bousahla, A.A., Bourada, F., Mahmoud, S.R., Tounsi, A., Algarni, A., Adda Bedia, E.A. and Tounsi, A. (2020), "Buckling and dynamic behavior of the simply supported CNT-RC beams using an integral-first shear deformation theory", *Comput. Concrete*, **25**(2), 155-166. https://doi.org/10.12989/cac.2020.25.2.155.

Boussoula, A., Boucham, B., Bourada, M., Bourada, F., Tounsi, A., Bousahla, A.A. and Tounsi, A. (2020), "A simple nth-order shear deformation theory for thermomechanical bending analysis of different configurations of FG sandwich plates", *Smart Struct. Syst.*, **25**(2), 197-218. https://doi.org/10.12989/sss.2020.25.2.197.

Boutaleb, S., Benrahou, K.H., Bakora, A., Algarni, A., Bousahla, A.A., Tounsi, A., Mahmoud, S.R. and Tounsi, A. (2019), "Dynamic Analysis of nanosize FG rectangular plates based on simple nonlocal quasi 3D HSDT", *Adv. Nano Res.*, **7**(3), 191-208. https://doi.org/10.12989/anr.2019.7.3.191.

Chaabane, L.A., Bourada, F., Sekkal, M., Zerouati, S., Zaoui, F.Z., Tounsi, A., Derras, A., Bousahla, A.A. and Tounsi, A. (2019), "Analytical study of bending and free vibration responses of functionally graded beams resting on elastic foundation", *Struct. Eng. Mech.*, **71**(2), 185-196. https://doi.org/10.12989/sem.2019.71.2.185.

Chikr, S.C., Kaci, A., Bousahla, A.A., Bourada, F., Tounsi, A., Adda Bedia, E.A., Mahmoud, S.R., Benrahou, S.R. and Tounsi, A. (2020), "A novel four-unknown integral model for buckling response of FG sandwich plates resting on elastic foundations under various boundary conditions using Galerkin's approach", *Geomech. Eng.*, **21**(5), 471-487. https://doi.org/10.12989/gae.2020.21.5.471.

Cong, P.H., An, P.T.N. and Duc, N.D. (2015), "Nonlinear stability of shear deformable eccentrically stiffened functionally graded plates on elastic foundations with temperature-dependent properties", *Sci. Eng. Compos. Mater.*, **24**(3), 1-15. https://doi.org/10.1515/secm-2015-0225.

Cong, P.H., Anh, V.M. and Duc, N.D. (2017), "Nonlinear dynamic response of eccentrically stiffened FGM plate using Reddy's TSDT in thermal environment", *J. Therm. Stresses*, **40**(6), 704-732. http://doi.org/10.1080/01495739.2016.1261614.

Draiche, K., Bousahla, A.A., Tounsi, A., Alwabli, A.S., Tounsi, A. and Mahmoud, S.R. (2019), "Static analysis of laminated reinforced composite plates using a simple first-order shear deformation theory", *Comput. Concrete*, **24**(4), 369-378. https://doi.org/10.12989/cac.2019.24.4.369.

Esmaeili, M. and Beni, Y.T. (2019), "Vibration and buckling analysis of functionally graded flexoelectric smart beam", *J. Appl. Comput. Mech.*, **5**(5), 900-917. https://doi.org/10.22055/JACM.2019.27857.1439.

Faleh, N.M., Ahmed, R.A. and Fenjan, R.M. (2018), "On vibrations of porous FG nanoshells", *Int. J. Eng. Sci.*, **133**, 1-14. https://doi.org/10.1016/j.ijengsci.2018.08.007.

Fenjan, R.M., Ahmed R.A. and Faleh, N.M. (2019a), "Investigating dynamic stability of metal foam nanoplates under periodic in-plane loads via a three-unknown plate theory", *Adv. Aircraft Spacecraft Sci.*, **6**(4), 297-314. https://doi.org/10.12989/aas.2019.6.4.297.

Fenjan, R.M., Ahmed, R.A., Alasadi, A.A. and Faleh, N.M. (2019a), "Nonlocal strain gradient thermal vibration analysis of double-coupled metal foam plate system with uniform and non-uniform porosities", *Coupled Syst. Mech.*, **8**(3), 247-257. https://doi.org/10.12989/csm.2019.8.3.247.

Fládr, J., Bílý, P. and Broukalová, I. (2019), "Evaluation of steel

fiber distribution in concrete by computer aided image analysis", *Compos. Mater. Eng.*, **1**(1),49-70. https://doi.org/10.12989/cme.2019.1.1.049.

Gafour, Y., Hamidi, A., Benahmed, A., Zidour, M. and Bensattalah, T. (2020), "Porosity-dependent free vibration analysis of FG nanobeam using non-local shear deformation and energy principle", *Adv. Nano Res.*, **8**(1), 49-58. https://doi.org/10.12989/anr.2020.8.1.049.

Gasik, M. (1995), "Scand. Ch226", *Acta Polytech.*, 72.

Ghadimi, M.G. (2020), "Buckling of non-sway Euler composite frame with semi-rigid connection", *Compos. Mater. Eng.*, **2**(1), 13-24. https://doi.org/10.12989/cme.2020.2.1.013.

Ghannadpour, S.A.M. and Mehrparvar, M. (2020), "Modeling and evaluation of rectangular hole effect on nonlinear behavior of imperfect composite plates by an effective simulation technique", *Compos. Mater. Eng.*, **2**(1), 25-41. https://doi.org/10.12989/cme.2020.2.1.025.

Ghiasian, S.E., Kiani Y., Sadighi, M. and Eslami, M.R., (2014), "Thermal buckling of shear deformable temperature dependent circular/annular FGM plates", *Int. J. Mech. Sci.*, **81**, 137-148. http://dx.doi.org/10.1016/j.ijmecsci.2014.02.007.

Hamad, L.B., Khalaf, B.S. and Faleh, N.M. (2019), "Analysis of static and dynamic characteristics of strain gradient shell structures made of porous nano-crystalline materials", *Adv. Mater. Res.*, **8**(3),179. https://doi.org/10.12989/amr.2019.8.3.179.

Hellal, H., Bourada, M., Hebali, H., Bourada, F., Tounsi, A., Bousahla, A.A. and Mahmoud, S.R. (2019), "Dynamic and stability analysis of functionally graded material sandwich plates in hygro-thermal environment using a simple higher shear deformation theory", *J. Sandw. Struct. Mater.* https://doi.org/10.1177/1099636219845841.

Hussain, M., Naeem, M.N., Khan, M.S. and Tounsi, A. (2020b), "Computer-aided approach for modelling of FG cylindrical shell sandwich with ring supports", *Comput. Concrete*, **25**(5), 411-425. https://doi.org/10.12989/cac.2020.25.5.411.

Hussain, M., Naeem, M.N., Taj, M. and Tounsi, A. (2020a), "Simulating vibrations of vibration of single-walled carbon nanotube using Rayleigh-Ritz's method", *Adv. Nano Res.*, **8**(3), 215-228. https://doi.org/10.12989/anr.2020.8.3.215.

Hussain, M., Naeem, M.N., Tounsi, A. and Taj, M. (2019), "Nonlocal effect on the vibration of armchair and zigzag SWCNTs with bending rigidity", *Adv. Nano Res.*, **7**(6), 431-442. https://doi.org/10.12989/anr.2019.7.6.431.

Jaesang, Y. and Addis, K. (2014), "Modeling functionally graded materials containing multiple heterogeneities", *Acta Mech.*, **225**(7), 1931-1943. https://doi.org/10.1007/s00707-013-1033-9.

Kaddari, M., Kaci, A., Bousahla, A.A., Tounsi, A., Bourada, F., Tounsi, A., Adda Bedia, E.A. and Al-Osta, M.A. (2020), "A study on the structural behaviour of functionally graded porous plates on elastic foundation using a new quasi-3D model: Bending and Free vibration analysis", *Comput. Concrete*, **25**(1), 37-57. https://doi.org/10.12989/cac.2020.25.1.037.

Kar, V.R. and Panda, S.K. (2016), "Nonlinear thermomechanical deformation behaviour of P-FGM shallow spherical shell panel", *Chin. J. Aeronaut.*, **29**(1), 173-183. https://doi.org/10.1016/j.cja.2015.12.007.

Kar, V.R. and Panda, S.K. (2020), "Nonlinear flexural vibration of shear deformable functionally graded spherical shell panel", *Steel Compos. Struct.*, **18**(3), 693-709. https://doi.org/10.12989/scs.2015.18.3.693.

Karami, B., Janghorban, M and Tounsi, A. (2019b), "On pre-stressed functionally graded anisotropic nanoshell in magnetic field", *J. Braz. Soc. Mech. Sci. Eng.*, **41**, 495. https://doi.org/10.1007/s40430-019-1996-0.

Karami, B., Janghorban, M. and Tounsi, A. (2019a), "Galerkin's approach for buckling analysis of functionally graded anisotropic nanoplates/different boundary conditions", *Eng. Comput.*, **35**, 1297-1316. https://doi.org/10.1007/s00366-018-0664-9.

Khiloun, M., Bousahla, A.A., Kaci, A., Bessaim, A., Tounsi, A. and Mahmoud, S.R. (2019), "Analytical modeling of bending and vibration of thick advanced composite plates using a four-variable quasi 3D HSDT", *Eng. Comput.*, 1-15. https://doi.org/10.1007/s00366-019-00732-1.

Kolahchi, R., Safaria, M. and Esmailpour, M. (2016), "Dynamic stability analysis of temperature-dependent functionally graded CNT-reinforced visco-plates resting on orthotropic elastomeric medium", *Compos. Struct.*, **150**, 255-265. https://doi.org/10.1016/j.compstruct.2016.05.023.

Kossakowski, P.G. and Uzarska, I. (2019), "Numerical modeling of an orthotropic RC slab band system using the Barcelona model", *Adv. Comput. Des.*, **4**(3), 211-221. https://doi.org/10.12989/acd.2019.4.3.211.

Lal, A., Jagtap, K.R. and Singh, B.N. (2017), "Thermo-mechanically induced finite element based nonlinear static response of elastically supported functionally graded plate with random system properties", *Adv. Comput. Des.*, **2**(3), 165-194. https://doi.org/10.12989/acd.2017.2.3.165.

Lee, N.J., Lai., G.S., Lau, W.J. and Ismail, A.F. (2020), "Effect of poly(ethylene glycol) on the properties of mixed matrix membranes for improved filtration of highly concentrated oily solution", *Compos. Mater. Eng.* **2**(1), 43-51. https://doi.org/10.12989/cme.2020.2.1.043.

Li, D., Deng, Z. and Xiao, H. (2016), "Thermomechanical bending analysis of functionally graded sandwich plates using four-variable refined plate theory", *Compos. B Eng.*, **106**, 107-119. http://doi.org/10.1016/j.compositesb.2016.08.041.

Li, D., Deng, Z., Chen, G., Xiao, H. and Zhu, L. (2017), "Thermomechanical bending analysis of sandwich plates with both functionally graded face sheets and functionally graded core", *Compos Struct.*, **169**, 29-41. http://doi.org/10.1016/j.compstruct.2017.01.026.

Matouk, H., Bousahla, A.A., Heireche, H., Bourada, F., Adda Bedia, E.A., Tounsi, A., Mahmoud, S.R., Tounsi, A. and Benrahou, K.H. (2020), "Investigation on hygro-thermal vibration of P-FG and symmetric S-FG nanobeam using integral Timoshenko beam theory", *Adv. Nano Res.*, **8**(4), 293-305. https://doi.org/10.12989/anr.2020.8.4.293.

Medani, M., Benahmed, A., Zidour, M., Heireche, H., Tounsi, A., Bousahla, A.A., Tounsi, A. and Mahmoud, S.R. (2019), "Static and dynamic behavior of (FG-CNT) reinforced porous sandwich plate using energy principle", *Steel Compos. Struct.*, **32**(5), 595-610. https://doi.org/10.12989/scs.2019.32.5.595.

Mishnaevsky, J.L. (2007), *Computational Mesomechanics of Composites*, John Wiley & Sons, U.K.

Mori, T. and Tanaka, K. (1973), "Average stress in matrix and average elastic energy of materials with misfitting inclusions", *Acta Metall.*, **21**(5), 571-574. https://doi.org/10.1016/0001-6160(73)90064-3.

Nemati, A.R. and Mahmoodabadi, M.J. (2019), "Effect of micromechanical models on stability of functionally graded conical panels resting on Winkler-Pasternak foundation in various thermal environments", *Arch. Appl. Mech.*, 1-33. https://doi.org/10.1007/s00419-019-01646-6.

Nguyen, D.D., Cong, P.H. and Quang, V.D. (2016), hermal stability of eccentrically stiffened FGM plate on elastic foundation based on Reddy's third-order shear deformation plate theory", *J. Therm. Stresses*, **39**(7), 772-794. http://dx.doi.org/10.1080/01495739.2016.1188638.

Nguyen, D.D., Nguyen, D.K. and Hoang, T.T. (2018) "Nonlinear thermo-mechanical response of eccentrically stiffened Sigmoid FGM circular cylindrical shells subjected to compressive and

uniform radial loads using the Reddy's third-order shear deformation shell theory", *Mech. Adv. Mater. Struct.*, **25**(13), 1156-1167. http://doi.org/10.1080/15376494.2017.1341581.

Nikkhoo, A., Asili, S., Sadigh, S., Hajirasouliha, I. and Karegar, H. (2019), "A low computational cost method for vibration analysis of rectangular plates subjected to moving sprung masses", *Adv. Comput. Des.*, **4**(3), 307-326. https://doi.org/10.12989/acd.2019.4.3.307.

Othman, M. and Fekry, M. (2018), "Effect of rotation and gravity on generalized thermo-viscoelastic medium with voids", *Multidisciplin. Model. Mater. Struct.*, **14**(2), 322-338. https://doi.org/10.1108/MMMS-08-2017-0082.

Ouakad, H.M., Sedighi, H.M. and Al-Qahtani, H.M. (2020), "Forward and backward whirling of a spinning nanotube nano-rotor assuming gyroscopic effects", *Adv. Nano Res.*, **8**(3), 245-254. https://doi.org/10.12989/anr.2020.8.3.245.

Panjehpour, M., Loh, E.W.K. and Deepak, TJ. (2018), "Structural Insulated Panels: State-of-the-Art", *Trends Civ. Eng. Archit.*, **3**(1) 336-340. https://doi.org/10.32474/TCEIA.2018.03.000151.

Parida, S. and Mohanty, S.C. (2017), "Thermoelastic vibration analysis of functionally graded skew plate using nonlinear finite element method", *J. Therm. Stresses*, **40**(9), 1111-1133. https://doi.org/10.1080/01495739.2017.1290513.

Ping, Z., Zhang, L.W. and Liew, K.M., (2014), "Geometrically nonlinear thermomechanical analysis of moderately thick functionally graded plates using a local Petrov-Galerkin approach with moving Kriging interpolation", *Compos. Struct.*, **107**, 298-314. https://doi.org/10.1016/j.compstruct.2013.08.001.

Pradhan, S.C. and Murmu, T. (2009), "Thermo-mechanical vibration of FGM sandwich beam under variable elastic foundations using differential quadrature method", *J. Sound Vib.*, **321**, 342-362. https://doi.org/10.1016/j.jsv.2008.09.018.

Rahmani, M.C., Kaci, A., Bousahla, A.A., Bourada, F., Tounsi, A., Adda Bedia, E.A., Mahmoud, S.R., Benrahou, K.H. and Tounsi, A. (2020), "Influence of boundary conditions on the bending and free vibration behavior of FGM sandwich plates using a four-unknown refined integral plate theory", *Comput. Concrete*, **25**(3), 225-244. https://doi.org/10.12989/cac.2020.25.3.225.

Ramirez, D., Cuba, L., Mantari, J.L., and Arciniega, R.A. (2019), "Bending and free vibration analysis of functionally graded plates via optimized non-polynomial higher order theories", *J. Appl. Comput. Mech.*, **5**(2), 281-298. https://doi.org/10.22055/JACM.2018.25177.1237.

Reddy, J.N. and Chin, C.D. (1998), "Thermomechanical analysis of functionally graded cylinders and plates", *J. Therm. Stresses*, **21**(6), 593-629. http://doi.org/10.1080/01495739808956165.

Refrafi, S., Bousahla, A.A., Bouhadra, A., Menasria, A., Bourada, F., Tounsi, A., Adda Bedia, E.A., Mahmoud, S.R., Benrahou, K.H. and Tounsi, A. (2020), "Effects of hygro-thermo-mechanical conditions on the buckling of FG sandwich plates resting on elastic foundations", *Comput. Concrete*, **25**(4), 311-325. https://doi.org/10.12989/cac.2020.25.4.311.

Reuss, A. (1929), "Berechnung der fliessgrenze von mischkristallen auf grund der plastizitätsbedingung für einkristalle", *J. Appl. Math. Mech.*, **9**, 49-58 (in German).

Rezaiee-Pajand, M., Masoodi, A.R. and Mokhtari, M. (2018), "Static analysis of functionally graded non-prismatic sandwich beams", *Adv. Comput. Des.*, **3**(2), 165-190. https://doi.org/10.12989/acd.2018.3.2.165.

Sahla, F., Saidi, H., Draiche, K., Bousahla, A.A., Bourada, F. and Tounsi, A. (2019), "Free vibration analysis of angle-ply laminated composite and soft core sandwich plates", *Steel Compos. Struct.*, **33**(5), 663-679. https://doi.org/10.12989/scs.2019.33.5.663.

Salah, F., Boucham, B., Bourada, F., Benzair, A., Bousahla, A.A. and Tounsi, A. (2019), "Investigation of thermal buckling properties of ceramic-metal FGM sandwich plates using 2D integral plate model", *Steel Compos. Struct.*, **33**(6), 805-822. https://doi.org/10.12989/scs.2019.33.6.805.

Salamat, D. and Sedighi, H.M. (2017), "The effect of small scale on the vibrational behavior of single-walled carbon nanotubes with a moving nanoparticle", *J. Appl. Comput. Mech.*, **3**(3), 208-217. https://doi.org/10.22055/jacm.2017.12740.

Sayyad, A. and Ghumare, S. (2019), "A new quasi-3D model for functionally graded plates", *J. Appl. Comput. Mech.*, **5**(2), 367-380. https://doi.org/10.22055/JACM.2018.26739.1353.

Sedighi, H.M., Daneshmand, F. and Abadyan, M. (2015), "Modified model for instability analysis of symmetric FGM double-sided nano-bridge: Corrections due to surface layer, finite conductivity and size effect", *Compos. Struct.*, **132**, 545-557. https://doi.org/10.1016/j.compstruct.2015.05.076.

Selmi, A. (2019), "Effectiveness of SWNT in reducing the crack effect on the dynamic behavior of aluminium alloy", *Adv. Nano Res.*, **7**(5), 365-377. https://doi.org/10.12989/anr.2019.7.5.365.

Semmah, A., Heireche, H., Bousahla, A.A. and Tounsi, A. (2019), "Thermal buckling analysis of SWBNNT on Winkler foundation by non local FSDT", *Adv. Nano Res.*, **7**(2), 89-98. https://doi.org/10.12989/anr.2019.7.2.089.

Shokrieh, M.M. and Kondori, M.S, (2020), "Effects of adding graphene nanoparticles in decreasing of residual stresses of carbon/epoxy laminated composites", *Compos. Mater. Eng.*, **2**(1), 53-64. https://doi.org/10.12989/cme.2020.2.1.053.

Sobhy, M. (2015), "Thermoelastic response of FGM plates with temperature-dependent properties resting on variable elastic foundations", *J. Appl. Mech.*, **7**(6), 1550082. https://doi.org/10.1142/S1758825115500829.

Taj, M., Majeed, A., Hussain, M., Naeem, M.N., Safeer, M., Ahmad, M., Khan, H.U. and Tounsi, A. (2020), "Non-local orthotropic elastic shell model for vibration analysis of protein microtubules", *Comput. Concrete*, **25**(3), 245-253. https://doi.org/10.12989/cac.2020.25.3.245.

Timesli, A. (2020), "An efficient approach for prediction of the nonlocal critical buckling load of double-walled carbon nanotubes using the nonlocal Donnell shell theory", *SN Appl. Sci.*, **2**, 407 (2020). https://doi.org/10.1007/s42452-020-2182-9.

Tlidji, Y., Zidour, M., Draiche, K., Safa, A., Bourada, M., Tounsi, A., Bousahla, A.A. and Mahmoud, S.R. (2019), "Vibration analysis of different material distributions of functionally graded microbeam", *Struct. Eng. Mech.*, **69**(6), 637-649. https://doi.org/10.12989/sem.2019.69.6.637.

Tounsi, A., Al-Dulaijan, S.U., Al-Osta, M.A., Chikh, A., Al-Zahrani, M.M., Sharif, A. and Tounsi, A. (2020), "A four variable trigonometric integral plate theory for hygro-thermo-mechanical bending analysis of AFG ceramic-metal plates resting on a two-parameter elastic foundation", *Steel Compos. Struct.*, **34**(4), 511-524. https://doi.org/10.12989/scs.2020.34.4.511.

Trinh, L.C., Vo, T.P., Thai, H.T. and Mantari, J.L. (2017), "Size-dependent behaviour of functionally graded sandwich microplates under mechanical and thermal loads", *Compos. B Eng.*, **124**, 218-241. https://doi.org/10.1016/j.compositesb.2017.05.042.

Trinh, M.C. and Kim, S.E. (2018), "Nonlinear stability of moderately thick functionally graded sandwich shells with double curvature in thermal environment", *Aerosp. Sci. Technol.*, **84**, 672-685. https://doi.org/10.1016/j.ast.2018.09.018.

Voigt, W., (1889), "Über die beziehung zwischen den beiden elastizitätskonstanten isotroper körper", *Wied. Ann. Phys.*, **38**, 573-587.

Yahiaoui, M., Tounsi, A., Fahsi, B., Bouiadjra Bouiadjra, R. and Benyoucef, S. (2018), "The role of micromechanical models in the mechanical response of elastic foundation FG sandwich thick beams", *Struct. Eng. Mech.*, **68**(1), 53-66. https://doi.org/10.12989/sem.2018.68.1.053.

Yoosefian, A.R., Golmakani, M.E. and Sadeghian, M. (2020), "Nonlinear bending of functionally graded sandwich plates under mechanical and thermal load", *Commun. Nonlin. Sci. Numer. Simul.*, **84**, 105161. https://doi.org/10.1016/j.cnsns.2019.105161.

Zarga, D., Tounsi, A., Bousahla, A.A., Bourada, F. and Mahmoud, S.R. (2019), "Thermomechanical bending study for functionally graded sandwich plates using a simple quasi-3D shear deformation theory", *Steel Compos. Struct.*, **32**(3), 389-410. https://doi.org/10.12989/scs.2019.32.3.389.

Zhu, P., Zhang, L.W. and Liew, K.M. (2014), "Geometrically nonlinear thermomechanical analysis of moderately thick functionally graded plates using a local Petrov-Galerkin approach with moving Kriging interpolation", *Compos. Struct.*, **107**, 298-314. https://doi.org/10.1016/j.compstruct.2013.08.001.

Zimmerman, R.W. (1994), "Behavior of the Poisson ratio of a two-phase composite material in the high-concentration limit", *Appl. Mech. Rev.*, **47**(1), 38-44. https://doi.org/10.1115/1.3122819.

Zuiker, J.R. (1995), "Functionally graded materials-choice of micromechanics model and limitations in property variation", *Compos. Eng.*, **5**(7), 807-819. https://doi.org/10.1016/0961-9526(95)00031-H.

CC